HHS Public Access

Author manuscript

Mol Pharm. Author manuscript; available in PMC 2019 March 26.

Published in final edited form as:

Mol Pharm. 2018 August 06; 15(8): 3595–3599. doi:10.1021/acs.molpharmaceut.8b00419.

Photosensitizer-encapsulated ferritins mediate photodynamic therapy against cancer associated fibroblasts and improve tumor accumulation of nanoparticles

Lu Li[1], **Shiyi Zhou**[2], **NingNing Lv**[1], **Zipeng Zhen**[2], **Tianji Liu**[1], **Shi Gao**[1], **Jin Xie**[2,3,*], and **Qingjie Ma**[1,*]

[1] Department of Nuclear Medicine, China-Japan Union Hospital of Jilin University, 126 Xiantai Street, ErDao District, Changchun 13033, China

[2] Department of Chemistry, University of Georgia, Athens, Georgia 30602, USA

[3] Bio-Imaging Research Center, University of Georgia, Athens, Georgia 30602, USA

Abstract

Nanoparticles have been widely tested as drug delivery carriers or imaging agents, largely due to their ability to selectively accumulate in tumors through the enhanced permeability and retention (EPR) effect. However, studies show that many tumors afford less efficient EPR effect and that many nanoparticles are trapped in the peri-vascular region after extravasation and barely migrate into tumor centers. This is to a large degree attributed to the dense tumor extracellular matrix (ECM), which functions as a physical barrier to prevent efficient nanoparticle extravasation and diffusion. In this study, we report a photodynamic therapy (PDT) approach to enhance tumor uptake of nanoparticles. Briefly, we encapsulate $ZnF_{16}Pc$, a photosensitizer, into ferritin nanocages, and then conjugate to the surface of the ferritin a single chain viable fragment (scFv) sequence specific to fibroblast activation protein (FAP). FAP is a plasma surface protein widely upregulated in cancer-associated fibroblast (CAF), which is a major source of the ECM fiber components. We found that the scFv conjugated and $ZnF_{16}Pc$ loaded ferritin nanoparticles (scFv-Z@FRT) can mediate efficient and selective PDT, leading to eradication of CAFs in tumors. When tested in bilateral 4T1 tumor models, we found that the tumor accumulation of serum albumin (BSA), 10 nm quantum dots (QDs), and 50 nm QDs, was increased by 2, 3.5, and 18 folds, after scFv-Z@FRT mediated PDT. Our studies suggest a novel and safe method to enhance the delivery of nanoparticles to tumors.

Keywords

fibroblast activation protein; cancer-associated fibroblast; photodynamic therapy; single chain viable fragment; ferritin; tumor penetration

* maqj@jlu.edu.cn and jinxie@uga.edu.

Author Contributions

The manuscript was written through contributions of all authors. All authors have given approval to the final version of the manuscript.

The authors declare no competing financial interest.

Supporting Information. The Supporting Information is available free of charge on the ACS Publications website.

INTRODUCTION

The past decade has witnessed fast progress in nanoparticle-based drug delivery.[1–3] Compared with small molecule drugs, which have short blood circulation half-lives, nanoparticles can stay long in the blood circulation, and selectively extravasate at the leaky tumor vasculature, leading to enhanced tumor accumulation (a.k.a. the EPR effect).[4–5] Such an improved tumor uptake leads to enhanced treatment outcomes and reduced systematic toxicity. One challenge, however, is that tumors often consist of a dense ECM,[6] which prevents efficient diffusion of nanoparticles.[5–6] This impediment is exacerbated by poorly organized tumor vessels and, associated with it, a high tumor interstitial fluid pressure (IFP).[6–7] Due to these reasons, many nanoparticles are trapped within the interstitial space of a tumor rather than migrating into its center.[7] This barrier limits nanoparticle delivery in many tumors. For nanoparticle-based drug delivery, even if the overall tumor uptake is improved, the treatment benefits can be limited due to inhomogeneous intratumoral drug distribution.[6, 8]

CAF is a major player behind the restricted penetration. CAFs are the main source of collagen, fibronectin, and vimentin in the tumor ECM.[9–10] CAFs secret fibers to form a complex meshwork, which, along with the imbedded stromal cells, constitute a physical barrier for macromolecules/nanoparticles.[10] CAF also secretes muscular fibers; the latter causes increased contractility[11] and an elevated IFP in solid tumors. It is reasoned that eliminating CAFs may reduce collagen contents in the ECM, leading to improved nanoparticle accumulation and diffusion. The challenge, however, is how to selectively eradicate CAFs without causing systematic toxicities. Herein we report a novel, ferritin-mediated PDT approach to solve the issue. Briefly, we encapsulate $ZnF_{16}Pc$, a photosensitizer, into the interior of a ferritin cage. Meanwhile, we conjugate a single chain variable fragment (scFv) that is specific to FAP[12] to the surface of the ferritin nanoparticles. FAP overexpression is found in CAFs of over 90% of epithelial tumors, but not in normal fibroblasts,[12] making it an excellent CAF biomarker. We intravenously (i.v.) injected the scFv conjugated and $ZnF_{16}Pc$ loaded ferritins (scFv-Z@FRT) into 4T1 bearing mice and applied photo-irradiation to tumor areas. We hypothesize that the enabled photodynamic therapy (PDT) can selectively kill CAFs, and this in turn will cause a reduced level of collagen in the tumor ECM. We injected bovine serum albumin (BSA) and quantum dots (QDs) as representative macromolecules or nanoparticles into the PDT treated mice, and examined their tumor accumulation to assess the impact of the PDT on nanoparticle delivery.

RESULTS AND DISCUSSION

Ferritins are protein cages found in many living organisms and their main function is iron storage.[13] Wild-type ferritins are a 24-mer assembly of both heavy- and light-chains.[14] In our study, however, we prepared recombinant rat ferritins that contain heavy-chain only. The protein expression and purification followed a protocol reported by us in a previous study.[15] Sodium dodecyl sulfate–polyacrylamide gel electrophoresis (SDS-PAGE) found a band at ~ 21 kDa (data not shown), which is in accordance with the reported molecular weight of the rat heavy-chain subunit.[14] Transmission emission tomography (TEM) found that each

ferritin nanoparticle has an external dimeter of ~ 12 nm and an internal diameter of ~ 8 nm. Dynamic light scattering (DLS) analysis revealed a hydrodynamic diameter at 12.0 ± 2.1 nm (Fig. 2a). These are also consistent with the previous reports.[16]

$ZnF_{16}Pc$ loading was achieved by exploiting the pH-mediated disassembly and reassembly of ferritin cages.[17] Briefly, we reduced the pH of a ferritin solution to ~2 to break the interaction between adjacent ferritin subunits. We added $ZnF_{16}Pc$ in DMSO into the solution, and then slowly tuned the pH back to neutral to induce nanocage reconstitution. $ZnF_{16}Pc$ was trapped within the reformed nanocages during the process suggested by no obvious change in size after loading (Fig. 2a). We passed the resulting mixture through a PD-10 desalting column to remove the unloaded $ZnF_{16}Pc$ molecules. The $ZnF_{16}Pc$ loading rate is dependent on the initial photosensitizer concentration.[18] In the present study, we added $ZnF_{16}Pc$ at a $ZnF_{16}Pc$:ferritin molar ratio of 120:1 to the ferritin solution. The resulting, $ZnF_{16}Pc$-loaded ferritins, or Z@FRT, has a photosensitizer loading rate of ~40 wt %. Notably, $ZnF_{16}Pc$ barely leaked out of the protein nanocage. This is because the molecule is hydrophobic and too bulky to easily pass through the ferritin surface channels.[19]

The FAP specific scFv sequence was reported in a previous study.[20] The DNA coding sequence was inserted into a pOPE101 plasmid, with a GGGGS spacer added to link the light and heavy chains.[21] Denatured SDS-PAGE found a band at ~26 kDa, confirming the successful production of the protein. The FAP scFv was coupled to the surface of Z@FRT using bis (sulfosuccinimidyl) suberate (BS3) as a crosslinker,[21] and the resulting scFv-Z@FRT conjugate was purified using a centrifugal filtration unit (MWCO=100 kDa) with a slight increase of size to 14.6 ± 2.0 nm (Fig. 2a). scFv-Z@FRT stayed precipitate-free in PBS up to 1 week as shown in Fig. 2b. Minimal quenching was observed with Z@FRT compared to free $ZnF_{16}PC$ (Fig. 2c).

We then examined the tumor tissue binding capacity of scFv-Z@FRT. For that purpose, we labeled scFv-Z@FRT with IRDye800 (ex/em = 780/800 nm). FAP is overexpressed in CAF of majority solid tumors.[22] It is expected that scFv-Z@FRT can bind to tumors of different types. Indeed, incubation of scFv-Z@FRT with tissue sections from primary 4T1 and LL/2 tumors as well as LL/2 metastasis in the liver all led to positive staining (Fig. 3). Meanwhile, when free scFv (30×) was applied simultaneously, the staining was efficiently blocked (Fig. 3). These results confirmed that scFv-Z@FRT can bind to different tumors through scFv-FAP interaction.

We conducted the PDT study in bilateral 4T1 tumor models. The animal model was established by subcutaneously injecting ~ 10^6 4T1 cells per site to both left and right hind limbs of each mouse. The *in vivo* experiments started when tumors reached a size of ~100 mm^3. We first i.v. injected scFv-Z@FRT to the animals (n = 3). A 671 nm laser (300 mW/cm^2, 15 min) was applied to the right-hand-side tumor 24 h later, with the left tumor covered by aluminum foil (Fig. 4a). After the treatment, the animals were euthanized and the tumors were sectioned and stained by anti-α-smooth muscle actin (α-SMA) antibodies. α-SMA is highly expressed in CAFs[23–24] and is a commonly recognized CAF marker. In the un-irradiated tumors, there was a high level of α-SMA positive staining (Fig. 4b). In the contralateral, irradiated tumors, on the other hand, the level of positive α-SMA staining was

dramatically decreased, suggesting the successful eradication of CAF. We also examined the contents of collagen in the tumor ECM by Mason's tricrhome staining (Fig. 4c). Compared to the un-irradiated tumors, the PDT-treated tumors showed a significantly reduced level of positive staining. This is because CAF is the main source of tumor collagen. Eliminating CAFs tipped the ECM hemostasis balance towards collagen degradation.

We then investigated the impact of PDT on tumor accumulation of macromolecules or nanoparticles. We tested this in the same bilateral 4T1 tumor models with the same irradiation protocol. Two days after the photo-irradiation, we i.v. injected BSA (~5 nm[25], IRDye800 labeled, 1 nmol), 10 nm PEGylated CdSSe/ZnS QDs (1 nmol, from Ocean Nanotech), or 50 nm PEGylated QDs (1 nmol, from Invitrogen), into animals. DLS analysis revealed the hydrodynamic diameters of the QDs as 10.7 ± 2.0 nm and 48.3 ± 12.0 nm, respectively (Fig. S1). We then tracked the nanoparticle migration on a Maestro II system. We observed gradual accumulation of the three probes in tumors on both sides. In all three cases, however, we found higher uptake of the probes in the irradiated tumors than in the contralateral tumors (Fig. 5).

After the 24 h imaging, we euthanized the animals, dissected both tumors, and performed *ex vivo* imaging on Maestro (Fig. 5). For BSA, the tumor update in the PDT-treated tumor was about twice that of the untreated tumor (2.0 ± 0.4). The amplitude of tumor uptake increase was 3.4 ± 0.5 fold for 10 nm QDs and 17.7 ± 0.9 fold for 50 nm QDs. These results suggest that the impact of the PDT-enhanced tumor uptake is size-dependent, and is more efficient for particles of a relatively large size.

We further examined the tumor issues by immunofluorescence staining (Fig. 6). For all three nanoparticles, we found significant amounts of signals outside of vasculature (stained by anti-CD31 antibody), suggesting efficient extravasation of macromolecules/nanoparticles. For 50 nm QDs, we found many nanoparticles were accumulated at the tumor peripheral region (Fig. 6). This suggests for relatively bulky nanoparticles, diffusion in tumors is still limited despite of PDT-induced ECM breakdown. For BSA, we found intensive signals not only at the peripheral margin but also in the central area of the tumor. Similarly, the 10 nm QDs showed overall uniform intratumoral distribution after PDT.

CONCLUSION

Overall, our studies show that anti-FAP PDT can be harnessed to improve nanoparticle accumulation and penetration in tumors. For relatively small nanoparticles, the treatment leads to a much more unique intratumoral distribution. For bulky nanoparticles, the relative tumor uptake was increased by more than 5 times after the PDT. Compared with antibody based photo-immunotherapy, where each molecule carriers a maximum of 5–10 photosensitizers, ferritins allow for a much higher photosensitizer loading rate (200 per nanocage) while affording a comparable particle size (~ 12 nm). The compact size, the specific scFv-FAP interaction, and the high $ZnF_{16}Pc$ loading works in conjugation to cause efficient CAF eradication. It is expected that this approach can work efficiently in other tumor types since most solid tumors have a high FAP expression. Meanwhile, further studies

are needed to optimize the PDT protocols and the time interval between PDT and nanoparticles administration for best EPR enhancement.

Supplementary Material

Refer to Web version on PubMed Central for supplementary material.

ACKNOWLEDGMENT

This work was supported by the National Natural Science Foundation of China (NSFC) projects (81771869, 81571708, and 81501506), the Technology Department of Jilin Province (20160101001JC), and the Norman Bethune Program of Jilin University (2015219). We also thank the funding support by the National Institutes of Health (R01EB022596, J.X., and R01NS093314, J.X.), the Congressionally Directed Medical Research Program (CA140666, J.X.), and the National Science Foundation (NSF1552617, J.X.),

REFERENCES

1. Panyam J; Labhasetwar V, Biodegradable nanoparticles for drug and gene delivery to cells and tissue. Adv. Drug. Deliv. Rev 2003, 55 (3), 329–47. [PubMed: 12628320]
2. Huang L; Li Z; Zhao Y; Yang J; Yang Y; Pendharkar Aarushi I; Zhang Y; Kelmar S; Chen L; Wu W; Zhao J; Han G, Enhancing Photodynamic Therapy through Resonance Energy Transfer Constructed Near-Infrared Photosensitized Nanoparticles. Adv. Mater 2017, 29 (28), 1604789.
3. Huang L; Li Z; Zhao Y; Zhang Y; Wu S; Zhao J; Han G, Ultralow-Power Near Infrared Lamp Light Operable Targeted Organic Nanoparticle Photodynamic Therapy. J. Am. Chem. Soc 2016, 138 (44), 14586–14591. [PubMed: 27786443]
4. Fang J; Nakamura H; Maeda H, The EPR effect: Unique features of tumor blood vessels for drug delivery, factors involved, and limitations and augmentation of the effect. Adv. Drug. Deliv. Rev 2011, 63 (3), 136–51. [PubMed: 20441782]
5. Maeda H, The enhanced permeability and retention (EPR) effect in tumor vasculature: the key role of tumor-selective macromolecular drug targeting. Adv. Enzyme. Regul 2001, 41, 189–207. [PubMed: 11384745]
6. Jain RK; Stylianopoulos T, Delivering nanomedicine to solid tumors. Nat. Rev. Clin. Oncol 2010, 7 (11), 653–64. [PubMed: 20838415]
7. Danhier F; Feron O; Preat V, To exploit the tumor microenvironment: Passive and active tumor targeting of nanocarriers for anti-cancer drug delivery. J. Control. Release 2010, 148 (2), 135–46. [PubMed: 20797419]
8. Brown JM; Giaccia AJ, The unique physiology of solid tumors: opportunities (and problems) for cancer therapy. Cancer Res. 1998, 58 (7), 1408–16. [PubMed: 9537241]
9. Tomasek JJ; Gabbiani G; Hinz B; Chaponnier C; Brown RA, Myofibroblasts and mechano-regulation of connective tissue remodelling. Nat. Rev. Mol. Cell. Biol 2002, 3 (5), 349–63. [PubMed: 11988769]
10. Kalluri R, The biology and function of fibroblasts in cancer. Nat. Rev. Cancer 2016, 16 (9), 582–98. [PubMed: 27550820]
11. Kalluri R; Zeisberg M, Fibroblasts in cancer. Nat. Rev. Cancer 2006, 6 (5), 392–401. [PubMed: 16572188]
12. Garinchesa P; Old LJ; Rettig WJ, Cell-Surface Glycoprotein of Reactive Stromal Fibroblasts as a Potential Antibody Target in Human Epithelial Cancers. P. Natl. Acad. Sci. U.S.A 1990, 87 (18), 7235–7239.
13. Harrison PM; Arosio P, The ferritins: molecular properties, iron storage function and cellular regulation. Biochim. Biophys. Acta 1996, 1275 (3), 161–203. [PubMed: 8695634]
14. Theil EC, Ferritin: structure, gene regulation, and cellular function in animals, plants, and microorganisms. Annu. Rev. Biochem 1987, 56, 289–315. [PubMed: 3304136]

15. Lin X; Xie J; Niu G; Zhang F; Gao H; Yang M; Quan Q; Aronova MA; Zhang G; Lee S; Leapman R; Chen X, Chimeric ferritin nanocages for multiple function loading and multimodal imaging. Nano Lett. 2011, 11 (2), 814–9. [PubMed: 21210706]

16. Tang W; Zhen ZP; Wang MZ; Wang H; Chuang YJ; Zhang WZ; Wang GD; Todd T; Cowger T; Chen HM; Liu L; Li ZB; Xie J, Red Blood Cell-Facilitated Photodynamic Therapy for Cancer Treatment. Adv. Funct. Mater 2016, 26 (11), 1757–1768.

17. Kim M; Rho Y; Jin KS; Ahn B; Jung S; Kim H; Ree M, pH-dependent structures of ferritin and apoferritin in solution: disassembly and reassembly. Biomacromolecules 2011, 12 (5), 1629–40. [PubMed: 21446722]

18. Zhen Z; Tang W; Guo C; Chen H; Lin X; Liu G; Fei B; Chen X; Xu B; Xie J, Ferritin nanocages to encapsulate and deliver photosensitizers for efficient photodynamic therapy against cancer. ACS Nano 2013, 7 (8), 6988–96. [PubMed: 23829542]

19. Yan F; Zhang Y; Yuan HK; Gregas MK; Vo-Dinh T, Apoferritin protein cages: a novel drug nanocarrier for photodynamic therapy. Chem. Comm 2008, (38), 4579–81. [PubMed: 18815689]

20. Brocks B; Garin-Chesa P; Behrle E; Park JE; Rettig WJ; Pfizenmaier K; Moosmayer D, Species-crossreactive scFv against the tumor stroma marker “Fibroblast activation protein” selected by phage display from an immunized FAP(−/−) knock-out mouse. Mol. Med 2001, 7 (7), 461–469. [PubMed: 11683371]

21. Zhen Z; Tang W; Wang M; Zhou S; Wang H; Wu Z; Hao Z; Li Z; Liu L; Xie J, Protein Nanocage Mediated Fibroblast-Activation Protein Targeted Photoimmunotherapy To Enhance Cytotoxic T Cell Infiltration and Tumor Control. Nano Lett. 2017, 17 (2), 862–869. [PubMed: 28027646]

22. Garin-Chesa P; Old LJ; Rettig WJ, Cell surface glycoprotein of reactive stromal fibroblasts as a potential antibody target in human epithelial cancers. P. Natl. Acad. Sci. U.S.A 1990, 87 (18), 7235–9.

23. Mueller MM; Fusenig NE, Friends or foes - bipolar effects of the tumour stroma in cancer. Nat. Rev. Cancer 2004, 4 (11), 839–49. [PubMed: 15516957]

24. Busch S; Acar A; Magnusson Y; Gregersson P; Ryden L; Landberg G, TGF-beta receptor type-2 expression in cancer-associated fibroblasts regulates breast cancer cell growth and survival and is a prognostic marker in pre-menopausal breast cancer. Oncogene 2015, 34 (1), 27–38. [PubMed: 24336330]

25. Kong G; Braun RD; Dewhirst MW, Hyperthermia enables tumor-specific nanoparticle delivery: effect of particle size. Cancer Res. 2000, 60 (16), 4440–5. [PubMed: 10969790]

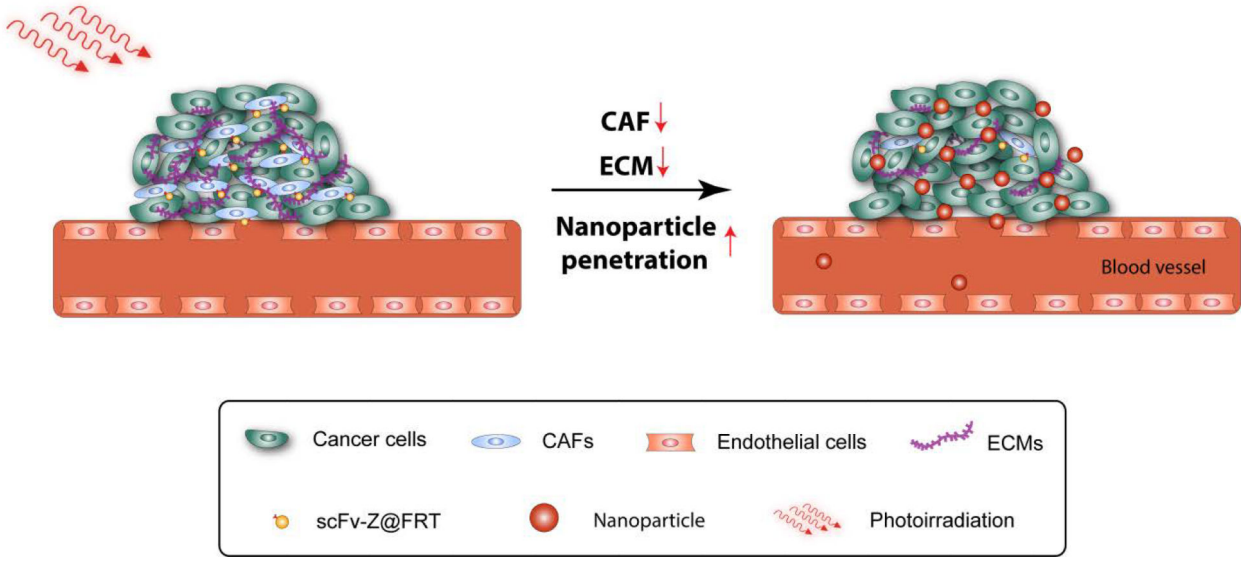

Figure 1.
Schematic illustration of CAF-targeted PDT to increase nanoparticle accumulation in tumor.

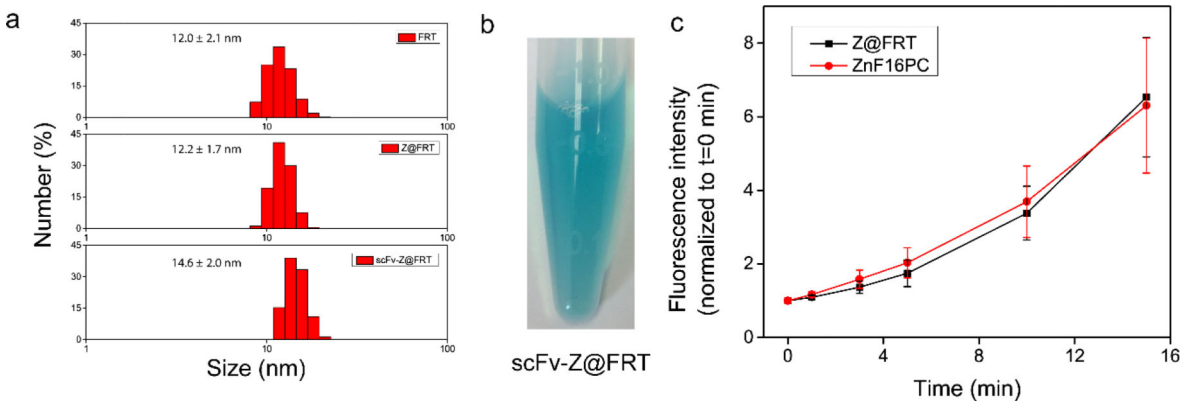

Figure 2.

a) DLS analysis of FRT, Z@FRT and scFv-Z@FRT. b) A photograph of scFv-Z@FRT in PBS. c) $^1O_2$ generation production, analyzed by Singlet Oxygen Green Sensor (SOSG) assay in 1% Tween 20/PBS solutions. A 671 nm laser at 0.1 W/cm^2 was applied to the solutions for 1, 3, 5, 10, and 15 min, and the 525 nm fluorescence was recorded and compared between Z@FRT and free $ZnF_{16}PC$.

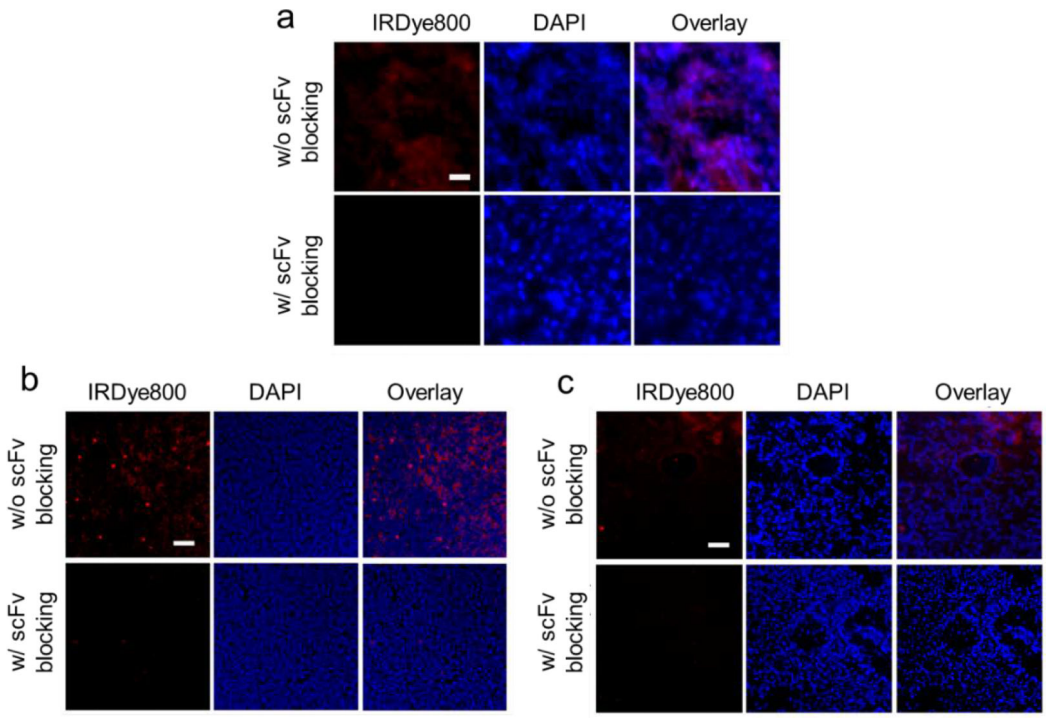

Figure 3.

Selective binding of scFv-Z@FRT against different tumor tissues. Tumor tissues were taken from a) subcutaneous 4T1 tumors, b) LL/2 metastasis in the liver, and c) LL/2 metastasis in the lung. The tumor tissues were stained with IRDye800 labeled scFv-Z@FRT and examined under a fluorescence microscope. For blocking studies, 30X free scFv was pre-incubated with the tumor tissues. The cell nuclei were stained with DAPI. Red, IRDye800 (scFv-Z@FRT); blue, DAPI. Scale bars: 100 μm.

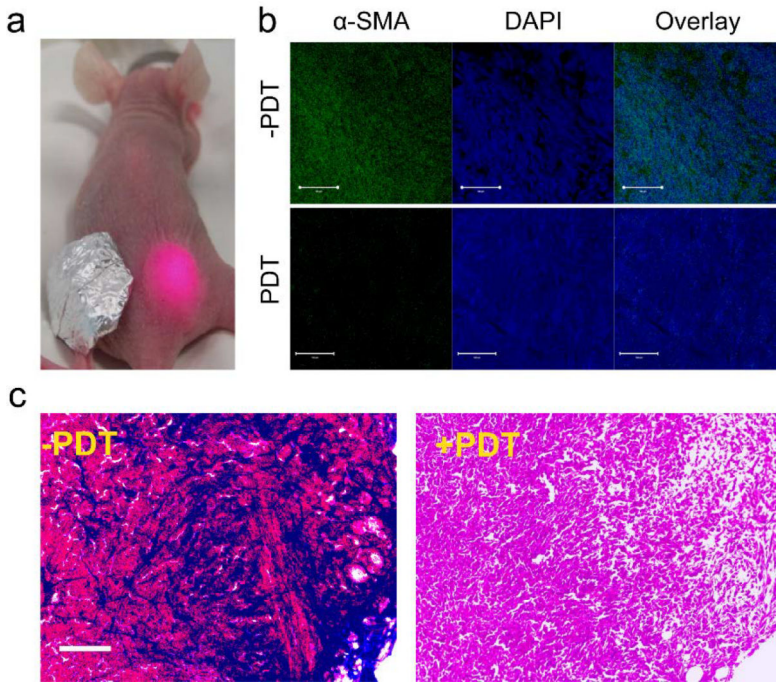

Figure 4.

PDT-induced CAF depletion. a) A photograph showing the setup of the PDT experiment. A 671 nm laser was applied to the right-hand-sided tumor at 24 h post scFv-Z@FRT injection. The left-hand-sided tumor was covered by aluminum foil. b) Confocal microscopic images of 4T1 tumor slices stained with FITC-conjugated anti-α-SMA antibody. Positive α-SMA staining was dramatically reduced two days after PDT. Green, FITC (α-SMA); blue, DAPI. Scale bars: 100 μm. c) Mason's trichrome staining results. Blue, collagen; red, muscle fibers; black/blue, nuclei.

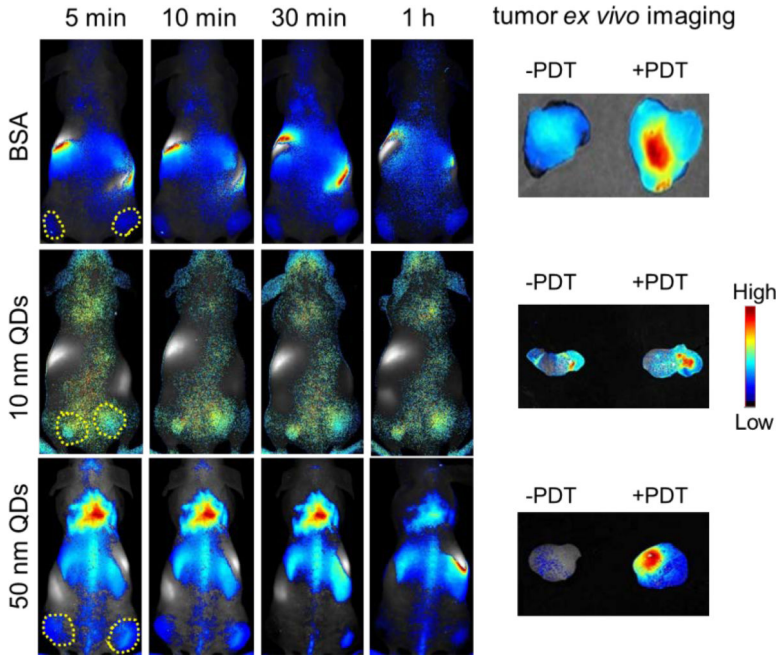

Figure 5.

In vivo and *ex vivo* imaging to assess the impact of scFv-Z@FRT mediated PDT on tumor accumulation of nanoparticles. Region of interest (ROI) analysis was performed to examine nanoparticle accumulation in the irradiated (right) and un-irradiated (left) tumors.

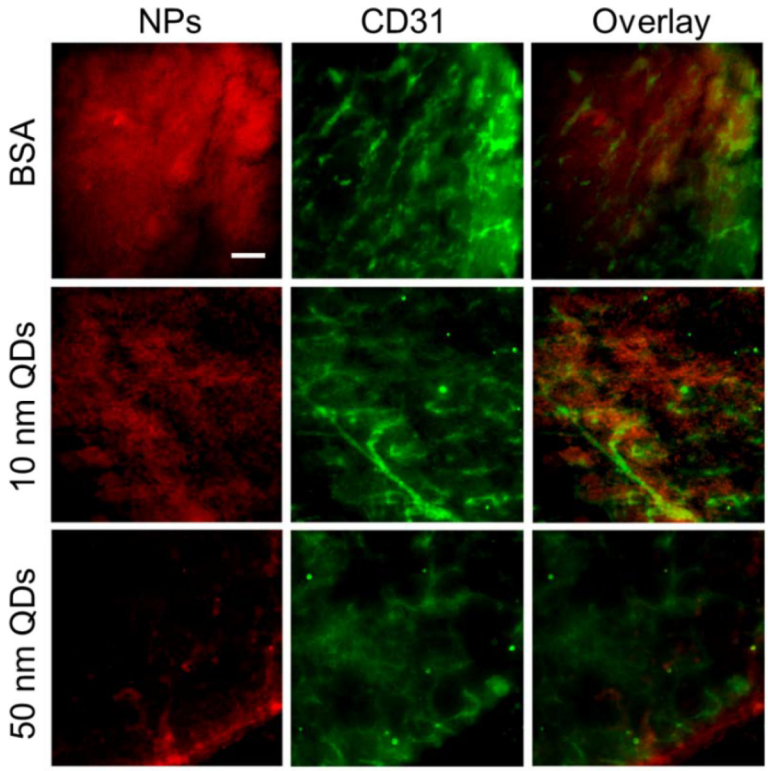

Figure 6.

Immunofluorescence imaging to examine nanoparticle diffusion in tumors after PDT. Significant extravasation was observed for BSA, 10 nm QDs, and 50 nm QDs. Red, IRDye800 (upper), 10 nm QDs (middle), or 50 nm QDs (lower). Green, blood vessels (CD31). Scale bar, 100 μm.